

# Massive black hole seeds from low angular momentum material

Savvas M. Koushiappas,<sup>1</sup> James S. Bullock,<sup>2\*</sup> Avishai Dekel,<sup>3</sup>

<sup>1</sup> *Department of Physics, The Ohio State University, 174 W. 18th Ave, Columbus, OH 43210 USA; smkoush@mps.ohio-state.edu*

<sup>2</sup> *Harvard Smithsonian Center for Astrophysics, 60 Garden St. Cambridge MA 02138 USA; jbullock@cfa.harvard.edu*

<sup>3</sup> *Racah Institute of Physics, The Hebrew University, Jerusalem, Israel; dekel@phys.huji.ac.il*

Released 2002 Xxxxx XX

## ABSTRACT

We present a cosmologically-motivated model in which the seeds of supermassive black holes form out of the lowest angular momentum gas in proto-galaxies at high redshift. We show that under reasonable assumptions, this leads naturally to a correlation between black hole masses and spheroid properties, as observed today. We assume that the gas in early-forming, rare-peak haloes has a distribution of specific angular momentum similar to that derived for the dark matter in cosmological N-body simulations. This distribution has a significant low angular momentum tail, which implies that every proto-galaxy should contain gas that ends up in a high-density disc. In haloes more massive than a critical threshold of  $\sim 7 \times 10^7 M_\odot$  at  $z \sim 15$ , the discs are gravitationally unstable, and experience an efficient Lin-Pringle viscosity that transfers angular momentum outward and allows mass inflow. We assume that this process continues until the first massive stars disrupt the disc. The seed black holes created in this manner have a characteristic mass of  $\sim 10^5 M_\odot$ , roughly independent of the redshift of formation. This serves as a lower bound for black-hole masses at galactic centers today. The comoving density of mass in black hole seeds grows with time, tracking the continuous production of critical mass haloes, and saturates when cosmic reionization acts to prevent gas cooling in these low-mass systems. By  $z \sim 15$ , the comoving mass density becomes comparable to that inferred from observations, with room for appropriate additional luminous growth during a later quasar accretion phase. The hierarchical merger process after  $z \sim 15$  naturally leads to a linear correlation between black-hole mass and stellar spheroid mass, with negligible black hole masses in disc-dominated galaxies. The formation of massive seeds at high redshifts, and the relatively important role of mergers in the buildup of today's black holes, are key elements in the proposed scenario.

**Key words:** cosmology – dark matter – galaxies: formation – galaxies: structure.

## 1 INTRODUCTION

Detailed studies of gas and stellar kinematics near the centers of present-day galaxies have revealed that almost all galaxy spheroids (ellipticals and bulges of spirals) host super-massive black holes, with masses  $M_{\text{bh}} = (10^6 - 10^9) M_\odot$ , or  $\sim 10^{-4}$  of the total stellar mass of their parent galaxies (e.g. Kormendy & Gebhardt 2001; Ferrarese & Merritt 2000; Magorrian et al. 1998). Although most of these black holes are not associated with quasar activity today, presumably they represent the now-dormant counterparts to the quasar-powering engines known to exist

at high redshift (Fan et al. 2001). Indeed, under reasonable assumptions, the luminosity function of Active Galactic Nuclei (AGN) can be explained by modeling mass accretion onto black holes that have the same range of masses as observed in local spheroids (see e.g. Steed & Weinberg 2003 and references therein). The standard expectation is that once a primordial galaxy is populated with a “seed” black hole at some early time, the black hole can grow via the accretion of available gas and, in the process, give off light in proportion to its Eddington luminosity.

The seed population is an important ingredient in any model that aims to explain AGN or local black holes, but the origin and nature of these objects remain unknown. In this paper, we provide a model for producing rather mas-

\* Hubble fellow

sive ( $\sim 10^{4-5} M_\odot$ ) seed black holes at early times from high density, low angular momentum gas in rare halos. We argue that massive, early forming seeds help explain the high redshift AGN population, and, unlike lower mass seeds, may give rise to the observed correlations between host galaxy properties and black hole masses without the need for fine-tuned feedback.

Consider, for example the analysis of Barth et al. (2003), who have estimated a mass of  $M_{\text{bh}} = (2 - 6) \times 10^9 M_\odot$  for a black hole powering a  $z = 6.4$  quasar found in the Sloan Digital Sky Survey. For the  $\Lambda$ CDM cosmology adopted below, the age of the universe at this redshift is 840 Myr. Even the remnant of a very massive, early-forming star of  $\sim 100 M_\odot$  would have to accrete mass at the Eddington limit for 17 e-folding times in order to grow to the observed mass. For a standard, thin-disk accretion model with an efficiency  $\sim 0.1$ , the e-folding Salpeter time is  $\sim 45$  Myrs, so an intermediate-mass seed would require 770 Myrs of accretion<sup>1</sup> in order to reach to observed mass, corresponding to a formation redshift for the seed of  $z_f \gtrsim 40$ . This is an extremely early redshift in the context of  $\Lambda$ CDM structure formation, since the minimum halo mass for  $\text{H}_2$  cooling at this time represents a  $\gtrsim 5\sigma$  fluctuation. While this does not completely rule out the possibility that the seed was small, it does require an extremely rare event. A  $10^5 M_\odot$  seed, on the other hand, would require  $\sim 10$  e-folding times of accretion, and thus a more recent formation redshift  $z_f \gtrsim 11$ . Of course these numbers are sensitive to certain assumptions, and may be influenced by allowing low efficiency accretion or super-Eddington luminosities. Nevertheless, it is generally easier to understand the population of  $z \gtrsim 6$  quasars if massive seeds are present (see also Haiman & Loeb 2001 for a related discussion).

Perhaps the most intriguing clues to the nature of black hole formation and growth are the strong correlations between black hole masses and global properties of their host spheroids — scales that differ by many orders of magnitude. The black hole mass is tightly correlated with the central velocity dispersion of the spheroid, and shows a significant correlation with the spheroid luminosity or mass. The theoretical challenge is to connect the galaxy-formation process originating on scales of megaparsecs with the black-hole formation processes on sub-parsec scales. In addition, the epoch of spheroid formation is likely much later than the time when the first quasar black holes begin to shine, so an additional challenge is to connect these two components in time, in a way that maintains, or even creates, the observed local correlations.

Several scenarios have been presented for the formation of massive black hole seeds. The general frameworks range from those that rely on the coalescence of massive stellar remnants that sink to the galaxy centers (Quinlan & Shapiro 1990; Hills & Bender 1995; Lee 1995; Ebisuzaki et al. 2001) to one that models black hole growth via ballistic particle capture during bulge collapse (Adams et al. 2001, 2003). Other models are based on the hydro-dynamical evolution of super-massive objects formed directly out of primor-

dial gas (Haehnelt & Rees 1993; Loeb & Rasio 1994; Eisenstein & Loeb 1995a; Haehnelt, Natarajan & Rees 1998; Gnedin 2001; Bromm & Loeb 2003). Our model is related most closely to this third type of scenario.

The key obstacle in any model of black hole formation is clearly the centrifugal barrier. In the standard cosmological framework of hierarchical structure formation, proto-haloes acquire angular momentum by tidal torques exerted by the background fluctuation field (Hoyle 1949; Peebles 1969; Barnes & Efstathiou 1987; Porciani, Delel & Hoffman 2002a,b). Haloes obtain a specific angular momentum that is on average 10 – 100 times smaller than that required for centrifugal support at the virial halo size (with a spin parameter of  $\lambda \sim 0.01 - 0.1$ , see below). This is roughly independent of mass and time. Thus, even after cooling, most of the gas can contract only to radii 10-100 times smaller than the initial halo radius before it is halted in circular orbits. The implied scale (at  $z = 0$ ) is  $\sim \text{kpc}$ , many orders of magnitude larger than the corresponding Schwarzschild radius,  $\sim 10^{-5} (M/10^9 M_\odot) \text{pc}$ . The situation may get even worse at earlier times because the typical collapsing mass  $M_*(a)$  is smaller in proportion to a high power of the expansion factor  $a \equiv (1+z)^{-1}$ . This implies that the ratio of the centrifugally supported size ( $\propto a M_*(a)^{1/3}$ ) to the Schwarzschild radius ( $\propto M_*(a)$  if the black hole mass is a constant fraction of the halo mass) increases dramatically at early times, unless the sites of black hole formation are rare haloes much more massive than  $M_*(a)$ . This line of argument indicates that the seed black holes originate from material at the very lowest end of the angular-momentum distribution within rare, massive haloes at high redshift. This material should then perhaps lose all its angular momentum via an effective mechanism of angular momentum transfer, which would be enhanced in such a high-density environment.

Eisenstein & Loeb (1995a) considered the sites of black hole formation to be the very high density discs which form in those rare haloes that have extremely low total angular momentum. Assuming a standard CDM scenario, they used an analytic model to predict the distribution of halo spins and estimated the abundance of haloes with low enough spin for efficient viscosity (Eisenstein & Loeb 1995b). They argued that there may be enough low-spin haloes to explain the black hole abundance. They then adopted the common view that viscosity in a differentially rotating gaseous disc is the mechanism that transfers angular momentum outward, thus allowing gas to contract into a black hole. In their calculations, they considered hydrodynamic (or perhaps hydro-magnetic) turbulence to be the viscous mechanism responsible for the angular momentum loss, and appealed to the  $\alpha$ -disc prescription (Shakura & Sunyaev 1973).

Our approach is related, but qualitatively different. We propose a scenario where seed black holes form from material with low angular momentum in all haloes that are massive enough to host an unstable self-gravitating disc. The required high-density discs can only occur in haloes that collapse at high redshift,  $z \gtrsim 10 - 20$ , when the angular momentum distribution of the (unprocessed) gas should be the most similar to that of the dark matter, and before reionization or some other feedback mechanism (e.g., Dekel & Silk 1986; Dekel & Woo 2003) prevents the growth of cold discs. The crucial point is that every halo, regardless of its total angular momentum, is expected to have a distribution

<sup>1</sup> This timescale is much larger than the estimated lifetimes of quasars at lower redshift (see Martini 2003 for a recent review).

of specific angular momentum including a tail of low-spin material.

The haloes we consider are massive enough so that the baryons trapped in their potential wells can cool and condense. In the absence of any other effect that may alter the angular momentum content of baryons, the lowest spin baryonic material in each system ends in a high-density central region forming a proto-galactic disc. As an illustrative fiducial model, we assume that the angular-momentum distribution in each halo matches the “universal” distribution of Bullock et al. (2001a) (B01 hereafter). If the angular momentum is approximately preserved during baryonic infall into the disk, the B01 angular momentum distribution implies that the inner disk becomes self gravitating with the surface density inversely proportional to the radius. We show below that if this behavior extends below the inner  $\sim 2\%$  of the disc radius, then enough mass may acquire a high enough density for viscosity to efficiently redistribute the angular momentum of the disc. For the final contraction of disc material into a black hole we evaluate the angular-momentum loss by the effective kinematic viscosity that arises from gravitational instabilities (Lin & Pringle 1987). This mechanism is somewhat more efficient than that from a typical  $\alpha$ -disc model. This viscosity-driven mass inflow cannot continue indefinitely; once the disc significantly fragments, or once it is heated or even disrupted by feedback, the inflow stops.

The semi-quantitative scenario presented here can be regarded as an illustration of a general model based on the assumption that proto-galactic gaseous discs develop high density inner regions dominated by low angular momentum material. Our current analysis is basically a feasibility study of such a model, and an attempt to recover its robust predictions and to constrain the model parameters by theoretical considerations as well as by the observations.

The outline of this paper is as follows. In § 2 we discuss the angular momentum distribution in proto-galaxies and the implied surface density profile for the cold discs. In § 3 we investigate the effect of kinetic viscosity on the evolution of the disc. In § 4 we calculate the resulting seed black hole mass and mass function. In § 5 we calculate the redshift evolution of the seed black hole mass density. In § 6 we make a preliminary attempt to address the correlation between the masses of black holes and galactic stellar spheroids, to be pursued in a subsequent paper. In § 7 we summarize our conclusions and discuss our results. When necessary, we assume a  $\Lambda$ CDM cosmology, with a Hubble constant  $h = 0.7$  ( $H_0 = 100h \text{ km s}^{-1} \text{ Mpc}^{-1}$ ), universal mass density  $\Omega_M = 0.3$ , cosmological constant  $\Omega_\Lambda = 0.7$ , and rms fluctuation amplitude  $\sigma_8 = 0.9$ .

## 2 SPIN DISTRIBUTION AND DISC PROFILE

We focus on the proto-galaxies forming in the redshift range  $z \sim 10 - 30$ . In the standard picture of structure formation, galaxies form as a uniform mixture of dark matter and baryons in small over-densities that grow by gravitational instability. Until its expansion turns around into a collapse, each halo acquires angular momentum through tidal torques induced by the density fluctuations around it. The dissipationless collapse brings the dark matter into virial equilibrium in an extended spheroidal halo. In the presence of an

efficient cooling mechanism, gas cools and condenses to a centrifugally supported disc.

Atomic line cooling can bring the gas to  $\sim 10^4 \text{ K}$ , and further cooling down to  $\sim 300 \text{ K}$  requires the presence of molecular hydrogen. The minimum halo mass for atomic cooling is  $M_a \simeq 6 \times 10^7 M_\odot [(1+z)/18]^{-3/2}$ , and for molecular hydrogen survival it is  $M_{H_2} \simeq 5 \times 10^6 M_\odot [(1+z)/18]^{-7}$  in the redshift range  $z \simeq 13 - 30$  (Tegmark et al. 1997; Abel et al. 1998). The haloes we consider below are just above the limit for atomic line cooling and significantly above the limit for molecular hydrogen cooling. We therefore expect the gas to cool and settle in an angular momentum supported disc on a timescale comparable to the dynamical time:

$$t_{\text{dyn}} \equiv (G\rho_{\text{vir}})^{-1/2} \simeq 77 \text{ Myr } \Delta_{178}(z)^{-1/2} \left( \frac{1+z}{18} \right)^{-3/2}, \quad (1)$$

where we have assumed our standard cosmological parameters and  $\Delta_{178}(z)$  is the virial overdensity in units of 178 times the background density.<sup>2</sup> Hereafter, due to the small redshift dependence of  $\Delta_{\text{vir}}$  at the redshifts of interest we set  $\Delta_{178}(z) = 1$ .

Consider a halo of virial mass  $M_v$  and spin parameter<sup>3</sup>  $\lambda \equiv J[\sqrt{2}M_v V_v R_v]^{-1}$ , where  $J$  is the total halo angular momentum. The virial radius is  $R_v = 384 \text{ pc } M_7^{1/3} [(1+z)/18]^{-1}$  and the virial velocity is  $V_v = 11 \text{ km s}^{-1} M_7^{1/3} [(1+z)/18]^{1/2}$ . Here,  $M_7 \equiv M_v/10^7 M_\odot$ . B01 found that in each halo the cumulative mass with specific angular momentum less than  $j$  is described well by the function

$$M(< j) = \mu M_v \frac{j}{j_0 + j}, \quad \mu > 1. \quad (2)$$

This profile has an implicit maximum specific angular momentum  $j_{\text{max}} = j_0/(\mu - 1)$ , where  $j_0 = \sqrt{2}V_v R_v \lambda/b(\mu)$ , with  $b(\mu) = -\mu \ln(1 - \mu^{-1}) - 1$ . The parameter  $\mu$  characterizes the shape of the angular momentum distribution. When  $\mu \rightarrow 1$  the deviation from a power law is pronounced with a larger fraction of the mass having low specific angular momentum, while if  $\mu \gg 1$  the distribution resembles a pure power law. The key property of this distribution is that at least half of the halo mass is in the power-law regime,  $M(< j) \propto j$ , and the simulations confirm that the power-law behavior extends at least over two decades in mass, down to  $\sim 1\%$  of the total halo mass.

The B01 profile was confirmed by Chen & Jing (2002) and Colín et al. (2002) using N-body simulations, and by van den Bosch et al. (2002), Chen, Jing & Yoshikawa (2003) and Sharma & Steinmetz (2003) using adiabatic hydrodynamic simulations. These studies reveal that the B01 angular momentum distribution remains a good fit to haloes at redshifts as high as  $z = 3$ . In what follows we will assume that

<sup>2</sup> If we use the approximation of spherical top-hat collapse given in Bryan & Norman (1998) we get  $\Delta_{\text{vir}}(z) \simeq (18\pi^2 + 82x - 39x^2)/\Omega_M(z)$ , where  $x + 1 = \Omega_M(z) = \Omega_M(1+z)^3/[\Omega_M(1+z)^3 + \Omega_\Lambda]$  and  $\Omega_M(z)$  is the ratio of the mean matter density to critical density at redshift  $z$ . In the  $\Lambda$ CDM cosmology that we adopt,  $\Delta_{\text{vir}}(z = 0) \simeq 337$  and  $\Delta_{\text{vir}}(z) \rightarrow 178$  at high redshift, approaching the standard CDM ( $\Omega_M = 1$ ) value.

<sup>3</sup> This spin parameter has been proposed by B01 as a practical modification of the conventional spin parameter, defined as  $\lambda = J\sqrt{|E|/GM_v^{5/2}}$ , where  $E$  is the halo energy. The two definitions of  $\lambda$  coincide for a singular isothermal sphere truncated at  $R_v$ .

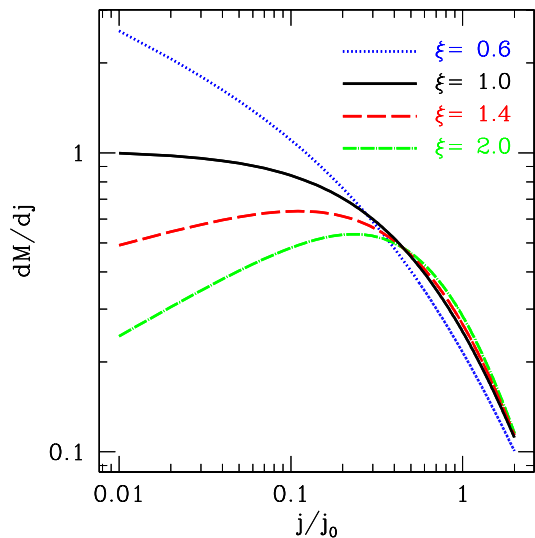


**Figure 1.** The mass per unit specific angular momentum for different values of the parameter  $\xi$ . Note that in our fiducial case of  $\xi = 1$  (B01), this function approaches a constant at small  $j$ .

the distribution holds at much higher redshifts,  $z \sim 15$ . Since the  $\Lambda$ CDM universe is effectively Einstein-de Sitter beyond  $z \sim 1$ , and the power spectrum is effectively a power law in the relevant mass range, one expects self-similarity between the haloes at  $z \sim 3$  and at  $z \sim 15$ . Therefore, the profile at  $z \sim 15$  can be assumed to resemble the B01 shape derived at  $z = 0$ . Simple theoretical considerations (B01, Dekel et al. 2000; Maller et al. 2002) argue that this angular momentum distribution is a natural outcome of the hierarchical clustering process. A qualitatively similar distribution is obtained when linear tidal torque theory is applied to haloes shell by shell, or when the orbital angular momentum of merging haloes turns into spin of the product halo via tidal stripping and dynamical friction. Other justifications follow from more detailed models (Maller & Dekel 2002; van den Bosch et al. 2001). These analytic models provide additional support to the assumption that a similar average halo profile is valid at low and high redshifts.

As mentioned above, the B01 distribution is a good fit to simulation results for angular momentum as small as  $\sim 1\%$  the characteristic angular momentum of the halo (corresponding to  $\sim 1\%$  the characteristic disc radius). As discussed below (see Eq. 13), our calculation assumes that the B01 form holds on scales below  $\sim 2\%$  of the characteristic angular momentum, so only a mild extrapolation of the low angular momentum tail is required, and being a power law, this extrapolation seems plausible. Nevertheless, the angular momentum distribution of the gas may not exactly mirror that of the dark matter. In order to evaluate the qualitative effects of this possibility and to explore alternative extrapolations, we will also consider deviations from the B01 distribution.

Unlike the analysis in B01 (but see Bullock et al. 2002), other works such as Chen & Jing (2002), van den Bosch et al. (2002) and Chen, Jing & Yoshikawa (2003) focused on estimating the fraction of dark mass with negative angular momentum (in the direction of the

total halo spin), and claimed that this fraction may be as large as  $\sim 20\%$ .<sup>4</sup> By using the B01 profile as is we actually adopt the conservative approach which minimizes the efficiency of black-hole formation, as follows. If a fraction of the gas starts with negative spin, it will mix dissipatively with the positive-spin gas leading to a purely rotating disc with no negative component. The implications on the disc formation depends on the way by which this mixing occurs. In the limiting case where the mixing occurs *after* the gas has already condensed to the disc, the negative component will mix positive spin material of exactly the same distribution of spin magnitudes. (van den Bosch et al. 2002). This results in a fraction of mass with near-zero angular momentum, which would increase the efficiency of black-hole production. If angular momentum mixing occurs during the process of gas cooling and collapse before the disc forms, there is no *a priori* reason for the negative angular momentum material to mix with only positive angular momentum material of the same magnitude. If this mixing is uniform across the angular momentum profile, then the resulting distribution should be similar to the B01 form, but with a slightly smaller overall spin parameter. The B01 form, ignoring the negative tail, is therefore the conservative case of minimum black-hole formation.

We assume that the specific angular-momentum distribution of the baryons resembles that of the dark matter halo. This assumption has been found to hold reasonably well in both radiative and non-radiative hydrodynamic simulations. (van den Bosch et al. 2002; Chen, Jing & Yoshikawa 2003). This assumption should be valid especially in systems that collapse early, as baryons would not have been affected by feedback associated with star formation. In addition we assume that the angular momentum of gas is conserved as gas cools and falls to the center forming a centrifugally supported disc. This assumption is backed by observations, where disc sizes seem to indicate that the angular momentum of the gas gained by tidal torques is retained. In addition, B01 found that the direction of angular momentum is well aligned at different radii, suggesting that the formation of a disc is indeed possible. Therefore, if there are no significant changes in the specific angular momentum of the baryons during the formation of the disc, then the disc angular-momentum distribution is  $M_d(< j) = f_0 M(< j)$ , where  $f_0$  is the final mass fraction in cold baryons. For the circular orbits in the disc one has  $j(r) = rV(r)$ , so one can map the  $M_d(< j)$  distribution to a radial mass profile in the disc. Note that if  $M_d(< j) \propto j$  (as with the B01 distribution at small  $j$ ) and the disc has a self-gravitating rotation curve  $V^2(r) \simeq GM_d(r)/r$ , then  $V(r) = \text{const.}$  and  $M_d(r) \propto r$  regardless of the initial properties of the halo and the possible effects of baryonic contraction on it. This implies a disc surface density profile of  $\Sigma(r) \propto r^{-1}$  in the inner disc. Since we expect these general trends to hold regardless of our assumptions about the halo profile, we make the simple approximation that the final total mass profile of halo plus disc follows that of an isothermal sphere, with  $M(r) \propto r$

<sup>4</sup> See the extensive discussion in B01 on the pitfalls that may arise when attempting to measure the negative fraction of material in dark halos.

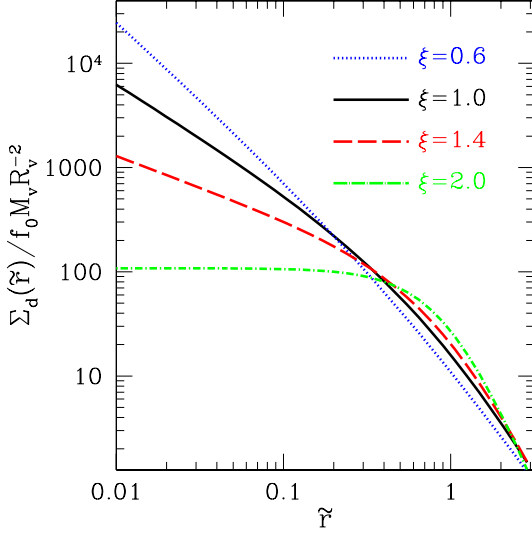


**Figure 2.** The disc surface density profile [eq. (6)] for different values of  $\xi$ . Our fiducial case,  $\xi = 1$ , shows a steep increase toward small radii, while the  $\xi = 2$  case has a flat core, similar to an exponential disc.

and  $V(r) = V_v$ . In this case, the disc mass profile implied by the distribution (2) is

$$M_d(\tilde{r}) = f\mu M_v \frac{\tilde{r}}{1 + \tilde{r}}, \quad \tilde{r} \equiv r/r_d, \quad (3)$$

where  $r_d$  is a characteristic disc radius,

$$r_d \equiv \frac{\sqrt{2}\lambda R_v}{b(\mu)} \simeq 22\text{pc } \lambda_{0.04} b(\mu)^{-1} M_7^{1/3} \left(\frac{1+z}{18}\right)^{-1} \quad (4)$$

and  $\lambda_{0.04} = \lambda/0.04$ . At  $r \ll r_d$ , we have again  $M_d \propto r$ . This profile is valid out to a maximum radius  $\tilde{r}_{\text{max}} = 1/(\mu - 1)$ . The constant  $f$  is the fraction of cold baryonic mass in the halo that has fallen into the disc by redshift  $z$  ( $f \leq f_0$ ).

Recall that it takes a finite time, of order  $\sim t_{\text{dyn}}$ , for a centrifugally supported disc to completely form after the baryons cool. Thus  $f$  in eq. (3) becomes equal to the total cold mass fraction  $f_0$  only after a time  $t \geq t_{\text{dyn}}$ . Before that time, we assume  $f = f_0(t/t_{\text{dyn}})$ , such that the disc mass grows linearly with time until  $t = t_{\text{dyn}}$ ,

$$M_d(t) = fM_v \simeq f_0 M_v \left(\frac{t}{t_{\text{dyn}}}\right), \quad 0 \leq t \leq t_{\text{dyn}}. \quad (5)$$

Hereafter we assume that the total cold mass fraction is  $f_0 = 0.03$ , which is roughly  $\sim 1/5$  of the universal baryon fraction of the standard  $\Lambda$ CDM Universe we assume in this paper (see also Klypin et al. 2002). This is a conservative estimate for the fraction of baryons that can form enough  $H_2$  to cool significantly (Tegmark et al. 1997; Abel et al. 1998).

Since our approach relies on an uncertain extrapolation of the B01 distribution, we explore a more general form for the angular momentum distribution, of which B01 is a special case. We consider the family of angular-momentum distributions that correspond to the following disc surface density profiles, parameterized by  $\xi$ ,

$$\Sigma_d(\tilde{r}) = \frac{Nf\mu M_v}{2\pi r_d^2} \frac{\xi \tilde{r}^{\xi-2}}{(1 + \tilde{r}^\xi)^2}, \quad \tilde{r} < (\mu - 1), \quad (6)$$

with the normalization constant  $N = \mu^{-1}[(\mu - 1)^\xi + 1]$ .

In Fig. 1 we show the differential angular momentum distributions for different values of  $\xi$ . The specific case of  $\xi = 1$  is the B01 form, while larger (smaller) values of  $\xi$  correspond to distributions with less (more) low angular momentum material. In Fig. 2 we show the resulting disc surface density profiles for different values of  $\xi$ . Note the steep increase in density for  $\xi = 1$  (B01), while for  $\xi = 2$  the density profiles are similar to an exponential disc.

Throughout this paper, we focus on the regime where  $\tilde{r} \ll 1$ , and the surface density is well-approximated by

$$\Sigma_d(\tilde{r}) \simeq \frac{N\xi f\mu M_v}{2\pi r_d^2} \tilde{r}^{\xi-2}. \quad (7)$$

We assume the B01 limit for the most part of this paper (which corresponds to  $\xi = 1$ ), but also investigate how our results change with varying the value of  $\xi$ .

### 3 ANGULAR MOMENTUM LOSS

After baryons cool and settle into a dense inner disc, angular momentum is redistributed as a result of viscosity. We adopt the kinematic viscosity prescription proposed by Lin & Pringle (1987) (see Laughlin & Rozyczka 1996 for a detailed test of this picture). According to this mechanism, global gravitational instabilities in the disc give rise to a transfer of angular momentum outward, which can be modeled as a local kinematic viscosity.

Consider a disc with local surface density  $\Sigma$ , angular frequency  $\omega$ , and temperature  $T$ , expressed as a sound speed  $c_s \simeq 2(T/300\text{K})^{1/2} \text{kms}^{-1}$ . As discussed by Toomre (1964), a disc is gravitationally unstable as long as the minimum size of shear-stabilizing disturbances  $L_s \simeq G\Sigma\omega^{-2}$ , is larger than the maximum size of dispersion-supported regions,  $L_d \simeq c_s^2 G^{-1} \Sigma^{-1}$ . This condition is expressed by evaluating the Toomre parameter  $Q$ ,

$$Q \equiv \left[\frac{L_d}{L_s}\right]^{1/2} \simeq \frac{c_s \omega}{G\Sigma}. \quad (8)$$

In discs with  $Q < 1$ , the interaction of the global instability perturbations with the background shear field drives a mass inflow. The transfer of angular momentum occurs across regions of maximum size  $\sim L_s$  over a typical timescale  $\gtrsim \omega^{-1}$  due to an effective viscosity

$$\nu \simeq \frac{L_s^2}{\omega^{-1}} \simeq \frac{G^2 \Sigma^2}{\omega^3}. \quad (9)$$

In what follows, we use  $\omega^2 = GM(r)r^{-3}$ .

A typical viscous time for mass inflow at a radius  $r$  in the disc is  $t_\nu \simeq r^2 \nu^{-1}$ . As mass flows in, the central regions of the disc become denser, so the value of  $Q$  decreases. If at any point  $Q$  became as small as  $Q^2 < H/r$ , where  $H \sim c_s/\omega$  is the height of the disc, then the instabilities would have become fully dynamical, fragmenting the disc into self-gravitating bodies, which would have stopped the angular momentum transfer. However, this effect is likely to be unimportant over the timescales of concern here because while  $Q$  is decreasing, the ratio  $H/r$  is actually decreasing at a faster rate (Mineshige & Umemura 1997), thus delaying the global fragmentation and allowing the viscosity to act until some external process disrupts the disc. The underlying assumption is that while the global instabilities give rise

to density waves, which cause the transfer of angular momentum, the disc does not fragment instantaneously. Star formation can occur concurrently with the viscous process until feedback from the first massive stars stops the gas inflow either by heating the disc or by disrupting it altogether (if its virial velocity is small enough).

### 3.1 Critical halo mass for viscous transport

Only haloes more massive than a critical minimum mass host unstable discs in which the angular-momentum loss is efficient and a seed black hole can form. This is because, from eq. (8), we expect  $Q \sim M^{-1/3}$ , implying a critical mass above which  $Q < 1$ . For the specific case of the B01 profile the scaling is  $Q \propto M_d^{-1/2} r_d^{1/2} \propto M_d^{-1/3} (1+z)^{-1/2}$ , independent of radius. If we assume  $M_d \leq f_0 M_v$ , then setting  $\xi = 1$  in eq. (7) yields a lower limit for host halo masses hosting  $Q < 1$  discs:

$$M_v^{\text{crit}} \geq 1.2 \times 10^7 M_\odot T_{300}^{3/2} \left( \frac{18}{1+z} \right)^{3/2} \times \left[ \left( \frac{\lambda}{0.04b(\mu)} \right) \left( \frac{0.03}{f_0} \right) \left( \frac{1.25}{\mu} \right) \right]^{3/2}. \quad (10)$$

All the quantities in brackets are of order unity, and  $T_{300} \equiv T/300 \text{ K}$  is the typical temperature for gas that has cooled via molecular Hydrogen.

A slightly improved estimate of this critical halo mass can be obtained by considering potential disc perturbations by major mergers during the gradual growth of disc mass until it reaches the baryon fraction  $f_0$  at  $t \sim t_{\text{dyn}}$  after virialization. If we approximate the rate of mass growth in the disc by eq. (5), then  $Q \propto M_d^{-1/3} \propto t^{-1/3}$  implies that initially self-gravity is negligible compared to gas pressure. As more material is accreted,  $Q$  decreases, and it may eventually reach  $Q \leq 1$  where angular momentum transfer begins. We define the timescale  $t_Q$  as the timescale needed for the disc to become gravitationally unstable had the accretion been uninterrupted. To evaluate this time, we assume that the disc is growing according to eq. (5), compute the surface density from the B01 profile (eq. (7) with  $\xi = 1$ ), and substitute in eq. (8) for  $Q$ . We then set  $Q = 1$  for the stability threshold and obtain

$$t_Q = 1.4 t_{\text{dyn}} T_{300} M_7^{-2/3} \left( \frac{18}{1+z} \right) \times \left( \frac{0.03}{f_0} \right) \left( \frac{1.25}{\mu} \right) \left( \frac{\lambda}{0.04b(\mu)} \right). \quad (11)$$

Figure 3 shows  $t_Q$  as a function of host halo mass at  $z = 17$  and at  $z = 13$ . We assumed the fiducial values  $\xi = 1$ ,  $T = 300 \text{ K}$ ,  $f_0 = 0.03$ ,  $\mu = 1.25$ , and  $\lambda = 0.04$ . These curves are compared to the virial dynamical times  $t_{\text{dyn}}$  at the two corresponding redshifts. The intersection of the  $t_Q$  and  $t_{\text{dyn}}$  curve marks the uninterrupted critical mass at that redshift, as estimated in eq. (10). However, a major merger may destroy the disc and disrupt the gas in-fall. If the typical time for a major merger to occur after the halo virializes is  $t_{\text{mm}}$ , the disc reaches a maximum mass of  $M_d \simeq (t_{\text{mm}}/t_{\text{dyn}}) f_0 M_v < f_0 M_v$ . In order to obtain a given critical disc mass where viscosity efficiently redistributes angular momentum, we require  $t_Q < t_{\text{mm}}$ , i.e., the disc should become self-gravitating *before* it gets disrupted. In this case,

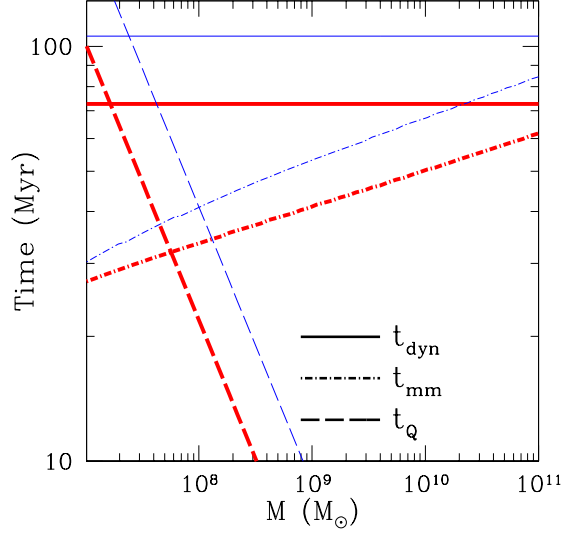


**Figure 3.** Timescales as a function of halo mass. Shown are (a) the time needed for the disc to become self-gravitating ( $t_Q$ ), (b) the time between virialization and the following major merger ( $t_{\text{mm}}$ ), and (c) the dynamical time ( $t_{\text{dyn}}$ ). Thick (red) lines correspond to  $z = 17$  and thin (blue) lines to  $z = 13$ . The critical mass for a halo that can form a seed black hole is determined by the intersection of the corresponding lines for  $t_Q$  and  $t_{\text{mm}}$ .

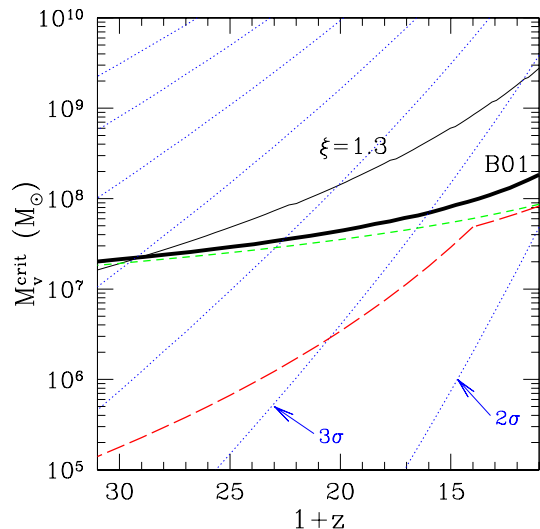
eq. (10) is an underestimate of the critical halo mass needed for disc instability that leads to efficient angular momentum transfer. In the regime we consider,  $t_{\text{mm}}$  is always less than  $t_{\text{dyn}}$ .

Figure 3 also shows the characteristic timescale for major mergers  $t_{\text{mm}}$ , in the extended Press-Schechter formalism (Press & Schechter 1974; Bond et al. 1991; Lacey & Cole 1993). Specifically, we associate  $t_{\text{mm}}$  with the peak of the probability distribution for the time it would take a halo to double its mass (see equation 2.21 in Lacey & Cole 1993). The intersection of the  $t_Q$  and  $t_{\text{mm}}$  curves (for a given redshift) marks the more realistic critical minimum mass, which turns out to be roughly a factor of  $\sim 4$  larger than the uninterrupted estimate (eq. 10).

Figure 4 shows  $M_v^{\text{crit}}$  calculated in the way just described as a function of redshift. The thick solid line was computed assuming the B01 profile for the gas density distribution. The redshift scaling is similar to that estimated in eq. (10), confirming that the critical mass is varying only slowly with redshift. The critical mass is about a factor of  $\sim 4$  larger than the uninterrupted estimate throughout the whole redshift range of interest. Shown for reference is the minimum halo mass for molecular hydrogen to survive as an efficient coolant; it justifies our assumption that gas can cool in critical-mass haloes.

Also shown in Fig. 4 is our estimated critical mass for a flatter surface density profile (or narrower angular-momentum distribution) with  $\xi = 1.3$ . As would be expected,  $M_v^{\text{crit}}$  is higher here than it is for the  $\xi = 1$  case. This is because densities at small radii are lower for a fixed mass disc, so a more massive host is needed in order to supply the extra disc mass required for  $Q < 1$ . Unfortunately, the instability calculation is less straightforward for  $\xi \neq 1$  because  $Q$  is not the same at all radii in the disc:





**Figure 4.** The minimum mass of a halo capable of forming a seed black hole as a function of redshift. The thick solid curve marked B01 refers to our fiducial  $\xi = 1$  distribution. The thin solid curve refers to  $\xi = 1.3$ , with a longer time of 20 Myr assumed for star formation. The dotted lines correspond to  $2\text{--}8\sigma$  fluctuations in the random fluctuation field, illustrating that the minimum masses of concern are rare systems. The short dashed line represents the minimum mass for atomic line cooling only, while the long dashed line is an approximation for molecular hydrogen cooling.

$Q \propto \tilde{r}^{(1-\xi)/2}$ . Indeed, for  $\xi > 1$  discs become unstable from the outside in; however, once inflow begins, mass transport always tends to increase the central density with time and therefore it is natural to assume that the central disc will become unstable within a viscous timescale. We can crudely estimate the critical mass in this case by evaluating  $Q$  and the viscous timescale at some characteristic radius. If we associate the viscous timescale with the timescale over which the disc would get disrupted (see next section), we can define the critical halo mass for black hole seed formation to be the mass scale at which  $Q < 1$  for the given viscous timescale. The  $\xi = 1.3$  curve in Fig. 4 has been computed assuming  $t = 20$  Myr. Despite the fact that this result relies on very crude approximations, it does serve to illustrate how narrower angular momentum distributions require more massive (and less abundant) haloes as the sites of black-hole formation. We come back to the implications of this later in the paper.

### 3.2 Viscous inflow

Consider now haloes more massive than the critical mass for disc instability and assume that they have formed discs with surface density profiles described by eq. (7). The viscous process transports mass inward from a radius  $r$  over the viscous time  $t_\nu \simeq r^2 \nu^{-1}$ . We make the assumption that if viscosity has been acting for time  $t$ , then all of the disc material originally within  $r_{\text{vis}} = (\nu t)^{1/2}$  has lost its angular momentum. Assuming a viscosity given by eq. (9), this

radius can be written as

$$\begin{aligned} \tilde{r}_{\text{vis}}^{3-\xi} &= 3.9 \times 10^{-4} N \xi^4 \left( \frac{f}{0.03} \right) \left( \frac{\mu}{1.25} \right) \left( \frac{0.04b(\mu)}{\lambda} \right)^3 \\ &\times \left( \frac{1+z}{18} \right)^3 \left( \frac{t}{\text{Myr}} \right)^2 \end{aligned} \quad (12)$$

where  $\tilde{r}_{\text{vis}} = r_{\text{vis}}/r_d$  and  $f = f_0(t_Q/t_{\text{dyn}})$ . For the special case of  $\xi = 1$ , we have

$$\begin{aligned} \tilde{r}_{\text{vis}} &= 1.9 \times 10^{-2} \left( \frac{f}{0.03} \right)^{1/2} \left( \frac{\mu}{1.25} \right)^{1/2} \left( \frac{0.04b(\mu)}{\lambda} \right)^{3/2} \\ &\times \left( \frac{1+z}{18} \right)^{3/2} \left( \frac{t}{\text{Myr}} \right) \end{aligned} \quad (13)$$

We see that the inflow radius grows linearly with the time available for viscosity to efficiently transfer angular momentum from the inner parts of the disc to outer radii.

According to the above equations, if the viscous angular-momentum transfer were to continue uninterrupted for a long enough time, then the whole disc would have eventually lost its angular momentum and collapsed. However as mentioned before, the major merger timescale sets an upper limit on the time available for this process, and in fact the feedback from star formation is likely to terminate the process even earlier.

In our adopted viscosity prescription, the first stars begin to form from the same instabilities that drive angular-momentum loss. Of course, if the disc completely fragments into stars then the angular momentum transfer stops, but the timescale for this is likely longer than the lifetimes of the very first massive stars. In addition, the presence of additional feedback on star formation, for example from magnetic fields, may play a role in setting this timescale (Gnedin 2001). Therefore, we assume that a more realistic estimate of the time available for viscosity to work is comparable to the timescale for collapse and evolution of the first self-gravitating bodies in the disc. These “first stars” should have very low metallicities because the haloes under consideration at  $z \sim 20$  had very few progenitors massive enough to have formed stars *before*  $z \sim 20$ . Thus, the stellar evolution in these stars is quite rapid, with lifetimes between  $\sim 1\text{--}30$  Myr, depending on many assumptions (Shapiro & Shibata 2002; Barafee et al. 2001; Heger & Woosley 2002; Shaerer 2002). We explore the range  $t = 1\text{--}30$  Myr for the time available for viscosity to transfer angular momentum away from the inner disc.

If angular momentum transfer is allowed to operate for a timescale  $t$ , then a large fraction of mass within  $\tilde{r}_{\text{vis}}$  would lose its angular momentum and form a central, massive object. This object would be pressure-supported and short-lived<sup>5</sup>, and inevitably collapse to a

<sup>5</sup> It is perhaps a concern that the presence of a pressure-supported object that grows over the viscous timescale might influence the temperature of the disc. We can estimate the heating of the disc if we assume that this object radiates at Eddington luminosity with an efficiency of  $\sim 0.1$  and that the disc is heated due to Thomson scattering. We find that it will take a time of order  $\sim 5t_{\text{vis}}$  to increase the temperature of the disc by 50% (this timescale is reduced to  $\sim 3t_{\text{vis}}$  if the object radiates at the Eddington limit). Since these timescales are greater than the viscous

black hole owing to the post-Newtonian gravitational instability (Shapiro & Teukolsky 1983). The exact mass of the resulting black hole depends on the mass loss experienced during the short lifetime of this “star”. This is an unknown quantity, but the mass loss is typically assumed to be in the range 10% – 90% of the initial mass of the object (Barafee et al. 2001; Heger & Woosley 2002; Shapiro & Shibata 2002). Hereafter we assume that the mass of the resulting black hole is some fraction  $\kappa$  of the total mass with zero angular momentum, and take  $\kappa = 0.5$  as our fiducial value where necessary.

#### 4 MASS FUNCTION OF SEED BLACK HOLES

We define the mass of the black hole  $M_{\text{bh}}$  as the fraction  $\kappa$  of the mass within  $\tilde{r}_{\text{vis}}(t)$ , i.e., the mass that lost its angular momentum over time  $t$ . Using equations (13) and (7) we obtain for the generalized profile

$$M_{\text{bh}} = 5 \times 10^{-4} M_v \left( \frac{\kappa}{0.5} \right) \left( \frac{\xi t}{\text{Myr}} \right)^{2\eta} \left( \frac{1+z}{20} \right)^{3\eta} \quad (14)$$

$$\times \left[ \frac{(N f \mu)^{1/\xi} b(\mu)}{\lambda} \right]^{3\eta} [20]^{3\eta-3/2} [1.1 \times 10^{-5}]^{2\eta-1},$$

where  $\eta \equiv \xi/(3-\xi)$ . For the B01 case with  $\xi = 1$  the result reduces to

$$M_{\text{bh}} = 3.8 \times 10^3 M_\odot \left( \frac{\kappa}{0.5} \right) \left( \frac{f}{0.03} \right)^{3/2} \left( \frac{\mu b(\mu)}{1.25} \right)^{3/2} \quad (15)$$

$$\times \left( \frac{\lambda}{0.04} \right)^{-3/2} \left( \frac{M_v}{10^7 M_\odot} \right) \left( \frac{1+z}{18} \right)^{3/2} \left( \frac{t}{\text{Myr}} \right)$$

Thus, for typical values, the black hole masses are quite large,  $\sim 10^4 M_\odot$ , and of order  $\sim 10^{-3}$  the mass of the host halo. Notice however that the black hole mass is quite sensitive to the value of the profile slope parameter  $\xi$  (e.g. the last term in eq. 14). For example, with  $\xi = 1.4$ , the black-hole mass is  $\sim 10^{-4}$  of the halo mass. A similar calculation using an exponential-like profile (with  $\xi = 2$ ) gives negligible seed black hole masses, unless the viscous timescale is much larger than the Hubble time at that high redshift.

In general, for a halo of a given mass  $M_v$  forming a black hole at redshift  $z$  we expect a spread in the parameters characterizing the distribution of angular momentum. We compute the conditional probability distribution of seed black hole masses given  $M_v$  at  $z$  for the  $\xi = 1$  case, where the distributions of the parameters  $\lambda$  and  $\mu$  are well-known. Note first that the black-hole mass scales as  $M_{\text{bh}} \propto [\mu b(\mu)/\lambda]^{3/2}$ , where we define for convenience  $\beta \equiv \mu b(\mu)$  and  $\gamma \equiv \beta/\lambda$ , such that  $M_{\text{bh}} \propto \gamma^{3/2}$ . The N-body simulations used by B01 show that the probability distributions of  $\lambda$  and  $\beta$  are well-parameterized by log-normal distributions of the form,

$$P(x)dx = \frac{1}{\sqrt{2\pi}\sigma_x} \frac{1}{x} \exp \left[ -\frac{\ln^2(x/x_0)}{2\sigma_x^2} \right] dx \quad (16)$$

timescales we consider here (set by the timescales for the formation and evolution of the first self-gravitating bodies in the disc) we conclude that the presence of this central short-lived object does not affect the thermal evolution of the disc.

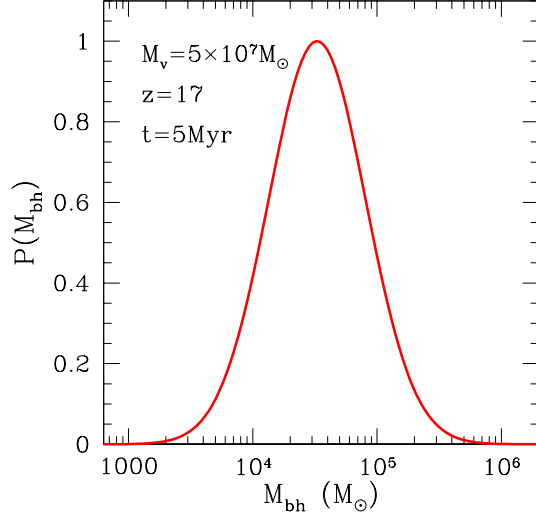


**Figure 5.** Probability distributions of seed black hole masses for the threshold halo mass at  $z = 17$ . The assumed angular-momentum distribution is  $\xi = 1$ , and the assumed viscosity timescale is 5 Myr.

where  $x_0 = 0.035, 1.25$  and  $\sigma_x = 0.5, 0.3$  for  $x = \lambda, \beta$  respectively. Given these distributions, it is easy to compute  $P(\gamma)$ , and from this the probability distribution of the seed black holes given for a halo of mass  $M_v$  at redshift  $z$  for a given viscous timescale  $t$ . The result is

$$P(M_{\text{bh}}|M_v) dM_{\text{bh}} = \frac{1}{\sqrt{2\pi}\sigma_{M_{\text{bh}}}} \frac{1}{M_{\text{bh}}} \times \exp \left[ -\frac{\ln^2(M_{\text{bh}}/M_{\text{bh}}^0)}{2\sigma_{M_{\text{bh}}}^2} \right] dM_{\text{bh}}. \quad (17)$$

where  $M_{\text{bh}}^0$  is

$$M_{\text{bh}}^0 = 3.8 \times 10^4 M_\odot \left( \frac{\kappa}{0.5} \right) \left( \frac{f}{0.03} \right)^{3/2} \left( \frac{M_v}{10^7 M_\odot} \right) \times \left( \frac{1+z}{18} \right)^{3/2} \left( \frac{t}{10 \text{ Myr}} \right) \quad (18)$$

and  $\sigma_{M_{\text{bh}}} = 0.9$ .

Figure 5 shows the seed black hole probability distribution normalized to a peak value of one, for a host halo of mass  $M_v = 5 \times 10^7 M_\odot$  at  $z = 17$  and a time available for angular momentum transfer  $t = 5$  Myr. In this case,  $t_{\text{dyn}}(z = 17) \approx 73$  Myr,  $t_Q(M = 5 \times 10^5 M_\odot, z = 17) \approx 35$  Myr and therefore  $f \approx 0.014$  yielding a mean seed black hole mass of  $M_{\text{bh}} \approx 3 \times 10^4 M_\odot$  with possible masses in the range  $10^3 - 10^6 M_\odot$ . Such a distribution function of seed black hole masses should provide a useful starting point for studies aimed at modeling the quasar properties within a cosmological context (Bromley, Somerville & Fabian 2003; Menou, Haiman & Narayanan 2001; Kauffmann & Haehnelt 2000) and can be used in of the merger history of supermassive black holes (Madau & Rees 2001; Volonteri, Haardt & Madau 2003).

Consider now black holes forming only in haloes of critical mass  $M_v^{\text{crit}}$ . If we approximate  $M_v^{\text{crit}}$  with equation (10), then the seed black hole given in equation (14) is indepen-



dent of redshift of formation, host halo mass, and spin parameter, and has a “universal” value of

$$M_{\text{bh}} \simeq 6 \times 10^4 M_{\odot} T_{300}^{3/2} \left( \frac{\kappa}{0.5} \right) \left( \frac{f_0}{0.03} \right)^{3/2} \left( \frac{t}{10 \text{ Myr}} \right). \quad (19)$$

However, it is expected that since  $M_{\text{v}}^{\text{crit}}$  depends on the spin parameter  $\lambda$  and  $\mu b(\mu)$  there will be a spread in the critical host halo masses. The critical mass  $M_{\text{v}}^{\text{crit}}$  scales as  $M_{\text{v}}^{\text{crit}} \propto \gamma^{-3/2}$ . If we use the probability distribution for  $P(\gamma)$  calculated as explained above, it is straightforward to calculate the distribution in the host halo masses. The result is a log-normal distribution with a mean of  $M_{\text{v}}^{\text{crit},0} \simeq 5 \times 10^7 M_{\odot} T_{300}^{3/2} [18/(1+z)]^{3/2}$  and a standard deviation of  $\sigma_{M_{\text{v}}^{\text{crit}}} = 0.9$ . Thus, if we focus on black holes forming within critical mass haloes only, our model predicts a near universal mass of  $\sim 10^5 M_{\odot}$ , with a log-normal distribution of the masses hosting these seeds.

## 5 TOTAL MASS IN SEED BLACK HOLES

In this section we calculate the comoving mass density of mass of seed black holes and make a comparison with the observed density of mass in black holes today in the local Universe. In this calculation we do not include any additional black hole growth via luminous accretion (which must occur at some level in order to match the observed quasar population). We therefore expect the calculated density to be smaller than the observed value. If, for example, most black holes experience a luminous accretion phase characterized by a few e-folding times, we want our cumulative mass density to fall below the locally observed black hole density by roughly an order of magnitude.

As halo masses grow with time, some haloes become more massive than the minimum mass threshold  $M_{\text{v}}^{\text{crit}}$  and become the sites of potential seed black hole formation. Since the threshold mass decreases only slowly with redshift (see figure 3.1), the mass density due to seed black holes is dominated by the seeds formed at the particular redshift of interest. Naturally, all haloes more massive than the critical host halo mass scale were able to form a seed black hole at some higher redshift. However, these mass scales correspond to higher-sigma fluctuations and therefore do not contribute significantly to the mass density. In order to include only the contribution coming from seed black holes formed in haloes that have just crossed the minimum mass threshold, we compare the typical growth rate of halo mass with the growth rate of  $M_{\text{v}}^{\text{crit}}$ . We find that the probability of a halo crossing the threshold having previously been massive enough to host black hole forming progenitors is vanishingly small ( $\sim 10^{-6}$ ). Therefore it is safe to assume that the contribution to the seed black hole mass density at each redshift comes predominantly from those seeds formed in haloes which have just crossed the minimum mass threshold near that particular redshift.

The comoving density of mass in black holes as a function of redshift can be determined by integrating over the formation rate of haloes at the threshold mass from some initial redshift  $z_i$  to the redshift of interest  $z$ , i.e.,  $\rho_{\text{bh}}(z) = \int_{z_i}^z (d\rho/dz) dz$ . We approximate the evolution in the co-moving number density of seed black holes, as

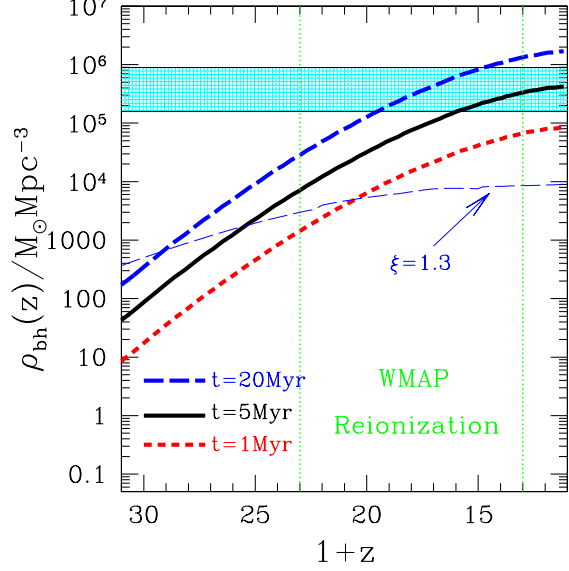


**Figure 6.** Total mass density in seed black holes as a function of redshift. Thick lines represent our fiducial  $\xi = 1$  (B01) angular-momentum distribution for various viscous timescales, while the thin line corresponds to  $\xi = 1.3$  and a viscous timescale of 20 Myr. The shaded area represents the observed range of total mass density in black holes at  $z = 0$ . The WMAP reionization range is marked by the vertical dotted lines.

$$\frac{d\rho(z)}{dz} = \frac{d}{dz} \left[ \int_{M_{\text{v}}^{\text{crit}}(z)}^{\infty} \frac{dn(z)}{dM} M_{\text{bh}}(M, z) dM \right]. \quad (20)$$

Here  $[dn(z)/dM]dM$  is the number density of haloes with mass in the interval between  $M$  and  $M + dM$  at redshift  $z$ , given by

$$\frac{dn(z)}{dM} dM = \frac{\rho_0}{M} f_1[\sigma(M), z] \left| \frac{d\sigma^2(M)}{dM} \right| dM \quad (21)$$

and  $\sigma(M)$  is the mean square fluctuation amplitude at a mass scale  $M$ . Here  $f_1$  is the fraction of mass associated with haloes of mass  $M$  corresponding to the given range in  $\sigma(M)$  at redshift  $z$ . We use the Press-Schechter (1974) approximation for  $f_1$  (see, e.g. Lacey & Cole 1993). Since the value of  $M_{\text{v}}^{\text{crit}}(z)$  is associated with increasingly higher sigma fluctuations at high redshifts, our results are not sensitive to the choice of  $z_i$ . We choose  $z_i = 30$ , but our results are unchanged for  $z_i = 50$ .

Figure 6 shows the comoving density of seed black holes obtained by integrating eq. (20). As expected, this function is strongly dependent on the time available for viscosity to redistribute angular momentum. At high  $z$  there is a rapid growth, which flattens off toward lower redshifts. The horizontal band marks the observationally-inferred density of mass in black holes today (Soltan 1982; Chokshi & Turner 1992; Kormendy & Richstone 1995; Fabian & Iwasawa 1999; Salucci et al. 1999; Merritt & Ferrarese 2001; Yu & Tremaine 2002). The total mass in black holes increases with time, until the cool gas supply stops due to some feedback mechanism that prevents and/or destroys the production of molecular hydrogen. Here we assume that cosmological reionization at  $z_{\text{re}}$  can be responsible for preventing the further cooling and collapse of haloes of

mass  $M_v^{\text{crit}}$  for redshifts  $z < z_{\text{re}}$ . This radiative feedback is expected to be especially effective in the relatively small systems under consideration. The  $\pm 1\sigma$  range for the redshift of reionization as measured by WMAP ( $z_{\text{re}} = 17 \pm 5$ , Spergel et al. 2003) is marked by the vertical lines. We expect the model prediction for the seed mass density at  $z_{\text{re}}$  to be roughly an order of magnitude below the accepted observed value today, in order to allow for the additional growth by accretion during an AGN phase. We see that for  $z_{\text{re}} = 17$ , say, this requirement is fulfilled once viscosity operates for a timescale of  $1 \leq t \leq 5 \text{ Myr}$ .

Also shown in Fig. 6 is the case  $\xi = 1.3$  with a viscous timescale of  $t = 20 \text{ Myr}$ . The curve is flatter in this case because  $M_v^{\text{crit}}$  for this profile grows faster than the  $\xi = 1$  case (see figure 4), and as a result the contribution from new seed black holes is smaller. In addition, the mass of the black hole associated with each halo above  $M_v^{\text{crit}}$  scales as  $\propto (1+z)^{3.8}$  for  $\xi = 1.3$  compared with  $\propto (1+z)^{1.5}$  for  $\xi = 1$  (see equation 15). We see that the model predictions for  $\xi = 1.3$  are acceptable only for long star-formation times,  $t \geq 20 \text{ Myr}$ . Flatter profiles, with  $\xi$  significantly larger than 1.3, either require a very long viscous timescale for seed formation, or they fail to produce enough mass in black holes by the mechanism proposed here. In this case one has only small early seeds and therefore must accrete for many e-folding times.

## 6 BLACK HOLES AND SPHEROIDS

Our model provides a prediction for massive seed black holes with a characteristic linear correlation between the masses of the seed black holes and their host haloes. In this section we show how our model for high-redshift seeds may lead naturally to a relation between the black hole mass and stellar spheroid mass at  $z = 0$  by following their evolution through halo merger trees. We associate a galaxy's disc mass with gas that is accreted as diffuse material since the last major merger event. Each incoming halo is assumed to host a mass of cold gas in its center, which can contribute to a spheroid component if the merger occurs on a short dynamical friction timescale. Similarly, if the merged halo hosts a black hole seed (see below) and reaches the central object in time, then this seed can merge with the central black hole. In this fiducial example, we assume that when black holes merge, their masses add linearly.

We generate halo merger trees using the algorithm developed by Somerville & Kolatt (1999) based on the extended Press-Schechter formalism (Press & Schechter 1974; Bond et al. 1991; Lacey & Cole 1993). According to this algorithm, the probability for a mass increase by  $\Delta M$  in a time step  $\Delta t$  is

$$P(\Delta\sigma^2, \Delta\delta_c) d(\Delta\sigma^2) = \frac{\Delta\delta_c}{\sqrt{2\pi}\Delta\sigma^3} e^{-\Delta\delta_c^2/2\Delta\sigma^2} d(\Delta\sigma^2), \quad (22)$$

where  $\Delta\delta_c = \delta_c(t) - \delta_c(t+\Delta t)$  is the linear fluctuation growth according to the chosen cosmological model, corresponding to the time step  $\Delta t$ , and  $\Delta\sigma^2 = \sigma^2(M) - \sigma^2(M+\Delta M)$  is the increment in mean-square fluctuation amplitude according to the given linear power spectrum, corresponding to the mass increment  $\Delta M$ . We choose the time step such that

$$\Delta\delta_c \leq \sqrt{M_{\text{min}} \frac{d\sigma^2(M)}{dM}} \quad (23)$$

for a chosen minimum halo mass  $M_{\text{min}}$ ; a mass increase by  $\Delta M < M_{\text{min}}$  is considered to be a smooth accretion process rather than a merger event. The merger tree is generated by randomly selecting progenitor masses according to the above probability distribution at each discrete time. The parent halo is identified with the most massive progenitor at each time while the rest of the mass is either in subhaloes or diffuse mass. The tree is truncated at a high redshift when the mass of the major progenitor is less than  $M_{\text{min}}$ . We run 50 Monte Carlo realizations of the merging histories for today's haloes in the mass range  $10^{11} - 10^{14} M_\odot$ , with  $M_{\text{min}} = 10^6 M_\odot$ .

For each merger, we take into account the finite time for the incoming subhalo to spiral in due to dynamical friction and reach the center of the host halo. We model each halo as a singular isothermal sphere with a radius and velocity given by the virial relations discussed in §2. The dynamical-friction time can then be written as (Binney & Tremaine 1987; Lacey & Cole 1993),

$$t_{\text{df}} = 0.42 \text{ Gyr} \left[ \frac{g(\epsilon, \eta)}{0.3} \right] \left( \frac{R}{\ln \Lambda} \right) \left( \frac{1}{1+z} \right), \quad (24)$$

where  $R$  is defined as the ratio of the mass of the major progenitor to the mass of the incoming halo. For our calculation we approximate the Coulomb logarithm as  $\ln \Lambda \simeq \ln R$ . The function  $g(\epsilon, \eta) = \epsilon^{0.5} \eta^2$  characterizes the effect that non-circular orbits have on the orbital decay (e.g. Tormen 1997; Ghigna et al. 1998). Here  $\epsilon$  characterizes the circularity of the orbit, and is defined as the ratio of the angular momentum of the orbit to the angular momentum of a circular orbit with the same energy. The parameter  $\eta$  characterizes the energy of the orbit by defining  $r_E = \eta R_v$  to be the radius of a circular orbit with the same energy as the actual orbit. We will adopt the typical parameters  $\eta = 0.6$  and  $\epsilon = 0.5$  (see, e.g., Zentner & Bullock 2003).

Material that ends up in a disc is assumed to be the gas that comes in as diffuse accretion since the last major merger. The last major merger is defined as a merger with an incoming object that is at least 50% the mass of the host. The diffuse gas may partly be the gas lost from dark haloes smaller than  $M \sim 2 \times 10^8 [(1+z)/18]^{-3/2}$  due to photo-evaporation starting at the epoch of reionization (e.g. Bullock et al. 2000; Shaviv & Dekel 2004). Although the gas escapes from the small haloes, it may remain bound to the larger host halo, and we assume that it is accreted onto the disc at about the same time the low-mass haloes are accreted. For haloes less massive than  $\sim 3 \times 10^{11} M_\odot$ , which roughly coincides with the upper limit for disc formation at high redshift, we indeed expect short infall times because of short cooling times and negligible shock heating (Birnboim & Dekel 2003).

The spheroid mass is assumed to be the straightforward sum of the cold baryons in the merged subhaloes throughout the merger history that sank to the center of the subhalo. We take the spheroidal component to be in place by the redshift of the last major merger assuming that a major merger would disrupt the system into an irregular galaxy. If the estimated sinking time of the incoming subhalo is shorter than the time interval between the subhalo merger and the last major merger we add to the bulge a mass  $f_0 M_s$ , where  $f_0 = 0.03$  is the assumed cold-gas fraction, and  $M_s$  is the mass of the merged halo. The choice of the mass fraction

in the definition of the major merger makes only a small difference to the final slope of the relation between black hole and spheroid mass, because the merger history tends to converge to the final mass after the last major merger.

Among the subhaloes that reach the center before the redshift of the last major merger, we determine if they have a black hole, and if so, we assume it merges with the central black hole over a short timescale. In principle, we could compute the black hole mass contained in each merged halo by following its full merger tree back in time, until some early redshift  $z \gtrsim z_{\text{re}}$ . However, since our aim is simply to investigate the ramifications of our scenario, we have chosen only to follow the merger tree of the most massive progenitor, and estimate the formation times of each merged subunit in a statistical fashion. This choice saves a significant amount of computational time.

Specifically, since seed black holes stopped forming at  $z = z_{\text{re}}$ , we can estimate the total black hole mass present in a subhalo of mass  $M_s$  that merges into the main host at a redshift  $z_{\text{mer}}$  by the following approximation. If  $z_{\text{mer}} < z_{\text{re}}$ , then the black-hole mass populating the merging subhalo is determined by integrating over the mass function of its progenitors at  $z_{\text{re}}$ ,

$$\begin{aligned}
 M_{\text{bh}} &= \int_{M_{\text{v}}^{\text{crit}}(z_{\text{re}})}^{\infty} \frac{M_s}{M} M_{\text{bh}}(M, z_{\text{re}}) \\
 &\times f_2[\sigma(M), z_{\text{re}} | \sigma(M_s), z_{\text{mer}}] \\
 &\times \left| \frac{d\sigma^2(M)}{dM} \right| dM.
 \end{aligned} \quad (25)$$

Here,  $M$  is the mass of progenitors. The function  $f_2[\sigma(M), z_{\text{re}} | \sigma(M_s), z_{\text{mer}}]$  represents the fraction of mass in haloes of mass  $M_s$  at  $z_{\text{mer}}$  that was in haloes of mass  $M$  at redshift  $z_{\text{re}}$  (see equation 2.15 of Lacey & Cole (1993)). The mass  $M_{\text{bh}}(M, z_{\text{re}})$  is the mass of the seed black hole residing in a halo of mass  $M$  at  $z_{\text{re}}$  according to eq. (15). If the merger occurs before  $z_{\text{re}}$ , then the black-hole residing in the merging subhalo is assumed to have a mass according to eq. (15), given the halo mass  $M_s$  at  $z_{\text{mer}}$ . We only need to follow the merger history back to the time when the major progenitor is as small as  $M_{\text{v}}^{\text{crit}}(z)$ , because when a progenitor is smaller than  $M_{\text{v}}^{\text{crit}}$ , no seed black holes will form.

The integral above gives only an average black hole mass for an ensemble of host haloes of mass  $M_s$ . So the approximation is valid if  $M_{\text{bh}} \gg M_0$ , where  $M_0$  is the seed mass associated with critical-mass haloes at  $z_{\text{re}}$ . However, for low-mass subhaloes, the approximation can break down because it allows solutions with black hole masses smaller than the initial seed masses,  $M_{\text{bh}} < M_0$  ( $\sim 6 \times 10^4 M_{\odot}$ , see Eq. 18). This is unphysical, because we assume that each black hole is built up by a series of mergers with seeds of mass  $M_0$ . We attempt to remedy this shortcoming in cases by randomly re-assigning the value of  $M_{\text{bh}}$  in these cases. Therefore if  $M_{\text{bh}} < M_0$  we choose a random uniform deviate  $r$ , and set  $M_{\text{bh}} = 0$  if  $r > M_{\text{bh}}/M_0$  and  $M_{\text{bh}} = M_0$  otherwise.

Figure 7 shows the resulting black-hole mass as a function of the host spheroid mass from the merger tree realizations described above (open symbols), in comparison with the observed data (solid points with errors, see caption). We have adopted model parameters of  $t = 10$  Myr and  $z_{\text{re}} = 15$ . The model predictions in the top panel refers to a given *fixed* halo mass today,  $M = 3.2 \times 10^{12} M_{\odot}$ , where only the ran-

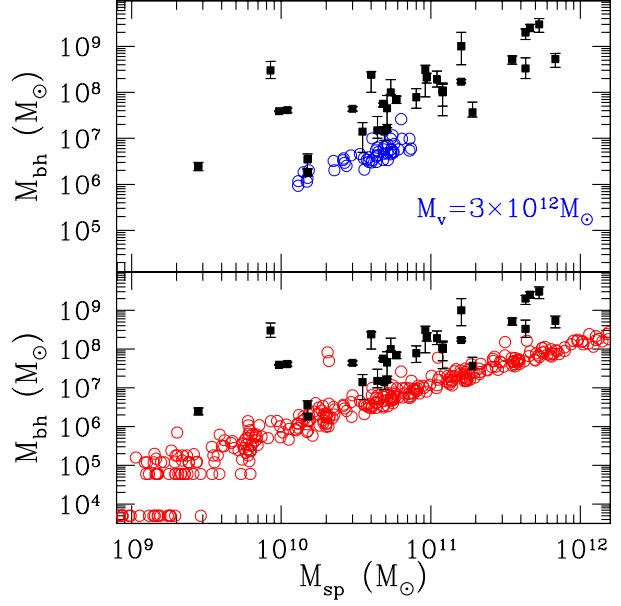


**Figure 7.** Today’s black-hole mass versus host-spheroid mass. The filled symbols are based on data from Tremaine et al. (2002), where the bulge mass is derived from the B absolute magnitude assuming the constant mass-to-light ratio advocated by van der Marel (1991). The model predictions are based on merger growth only, ignoring accretion. Top: for a fixed halo mass today,  $M_v = 3.2 \times 10^{12} M_{\odot}$ , using 50 random realizations of the merger tree. The variations in merger history by themselves tend to spread the masses along the observed relation. Bottom: for a range of present halo masses,  $M_v = 10^{11} - 10^{13.5} M_{\odot}$ , with logarithmic half order of magnitude steps. The slope of the predicted relation is in agreement with the observed slope. In cases where the black-hole mass is calculated to be zero, we have placed the symbol at the bottom of the panel for clarity. The predicted black-hole masses could potentially increase by about an order of magnitude due to accretion in an AGN phase.

dom merger history is varied from point to point. Though not shown, the associated disc masses for these haloes range from  $10^{10} - 10^{11} M_{\odot}$  with no clear correlation between the disk and black hole masses.

We find that the black hole mass correlates with the mass of the spheroid component, as observed, even for a fixed-mass host halo. This result arises because subhaloes that are massive enough to sink to the center of the parent halo and contribute to a bulge, are generally massive enough to host black holes as well. Haloes which experienced many mergers with small subhaloes tend to have a small spheroids and small black holes. This would naturally explain why black hole mass is observed to correlate with spheroid mass and not disc mass (Gebhardt et al. 2001), since disc mass does not correlate well with the merger history in our picture.

The bottom panel of Fig. 7 shows several ensemble realizations for a series of host halo masses with  $z = 0$  values of  $10^{11} - 10^{13.5} M_{\odot}$ . The computed relation follows closely  $M_{\text{bh}} \propto M_{\text{sp}}$ , and is qualitatively similar to the observed relation at  $z = 0$ . The normalization (set primarily in this case by setting  $t = 10$  Myr) allows for an additional growth by a few e-folds during an AGN accretion phase, as desired.

In addition, for the lowest-mass spheroids, we see in some cases the absence of any black hole mass (points along the bottom edge represent  $M_{\text{bh}} = 0$ ). This comes about because low mass host haloes are less likely to have had progenitors more massive than  $M_{\text{v}}^{\text{crit}}$  at  $z = z_{\text{re}}$ . Black holes cannot be smaller than the characteristic seed mass  $\sim 6 \times 10^4 M_{\odot}$  while there is no fixed mass threshold for a progenitor to contain gas that will eventually end up in a spheroid. This gives rise to a slightly steeper slope in the bottom left of the relation. The apparent increase in the number of low mass spheroids with no black holes also suggests the presence of a lower mass limit on spheroids hosting black holes, of roughly  $M_{\text{sp}} \sim 10^8 M_{\odot}$ . This is a potentially verifiable prediction of the model.

It is of interest to investigate the robustness of the derived relation between  $M_{\text{bh}}$  and  $M_{\text{sp}}$  to specific assumptions of the model presented here. For example, the result is practically independent of the finite duration of a merger due to dynamical friction. Major mergers are quick and have an immediate effect on the growth rate of the spheroid as well as the black hole, while minor mergers take a long time to complete and therefore have a delayed effect that may not materialize in a Hubble time (Zentner & Bullock 2003; Taylor & Babul 2001, 2003). When we repeat the calculation under the assumption that *all* mergers are instantaneous, ignoring the finite duration of the spiral-in process, we find that the predicted relation between black holes and spheroids remains almost unchanged, with only a slight shift of typically less than 10% towards larger spheroid masses for the same black hole mass. This small shift is to be expected since the less massive subhaloes that now contribute to the spheroid mass tend to be below the critical mass for seed formation and thus do not add to the black hole mass.

We find the predicted slope of the relationship to be insensitive to the actual value of  $M_{\text{v}}^{\text{crit}}$  (as long as  $M_{\text{v}} \gg M_{\text{v}}^{\text{crit}}$ ). The normalization of the relation, namely the black-hole mass for a given spheroid mass, is roughly inversely proportional to  $M_{\text{v}}^{\text{crit}}$ . This is because for a lower value of  $M_{\text{v}}^{\text{crit}}$  more haloes are able to form a seed and contribute to the merged black-hole mass without affecting the spheroid mass.

We also find that the slope is insensitive to the value of  $z_{\text{re}}$  (as long as  $z_{\text{re}} \geq 6$ ), while the normalization does depend on it. For a lower  $z_{\text{re}}$ , seed formation takes place in a larger fraction of the haloes that eventually merge to form spheroids. By lowering  $z_{\text{re}}$  from 15 to 6 we obtain an order of magnitude increase in black-hole mass. A comparable decrease in black-hole mass is obtained when increasing  $z_{\text{re}}$  from 15 to 20.

However, the slope of the relation is found to be mildly sensitive to the original scaling between the seed black hole mass and its host halo mass. If we replace the predicted correlation of our model ( $M_{\text{bh}} \propto M_{\text{v}}$ ) with an ad hoc seed assignment to critical-mass haloes at high redshift, e.g.,  $M_{\text{bh}} \propto (M_{\text{v}}^{\text{crit}})^3$ , we find that the linear  $M_{\text{bh}} \propto M_{\text{sp}}$  relation steepens to roughly  $M_{\text{bh}} \propto M_{\text{sp}}^{3/2}$ . This is because the ratio  $M_{\text{bh}}/M_{\text{v}}$  is now monotonically increasing with  $M_{\text{v}}$ . This mild sensitivity means that the predicted correlation of our physical model for seeds is important, but it does not have to be exactly  $M_{\text{bh}} \propto M_{\text{v}}$ .

Finally, we point out that our result is quite sensitive

to the way we assign mass  $M$  to a black hole which results from the merger of two black holes, of masses  $M_1$  and  $M_2$ . In our fiducial calculation we have assumed that the black hole masses sum up linearly,  $M = M_1 + M_2$ . On the other hand, if entropy is conserved, the mass of the merger product is  $M = \sqrt{M_1^2 + M_2^2}$  (Hawking 1971a,b). This should serve as a lower bound to the possible mass of the merger product, and should yield the flattest-possible  $M_{\text{bh}} - M_{\text{sp}}$  relation. Consider a black hole in the center of the halo formed from  $N_{\text{m}}$  mergers of seed black holes of mass  $M_{\text{bh}} \sim 10^5 M_{\odot}$ . If entropy is conserved, and  $N_{\text{m}} \gg 1$  then the black hole mass would be  $M_{\text{bh}} = M_{\text{seed}}(1 + N_{\text{m}})^{1/2} \propto N_{\text{m}}^{1/2}$ . In our model, spheroids grow via a series of mergers with the gas from nearly equal-mass haloes, roughly as  $M_{\text{sp}} \simeq f_0 M_s N_{\text{m}} \propto N_{\text{m}}$ , so we expect  $M_{\text{bh}} \propto M_{\text{sp}}^{1/2}$  in this limit. When we follow this recipe for mass adding using our full merger-tree method, we indeed obtain a result very close to our expectation:  $M_{\text{bh}} \propto M_{\text{sp}}^{0.55}$ . Thus, in this limit, the derived relation would be somewhat flatter than observed. In order to comply with the observed relation, one would have to appeal to a scenario where black-hole growth via accretion is more efficient in high-mass spheroids (e.g., Volonteri, Haardt & Madau 2003).

With the above tests in mind, we conclude that the derived linear relation between black hole and spheroid mass depends primarily on the fact that the seeds were massive, that they formed at high redshift, and that their masses add roughly linearly when they merge. In this case the build-up of black holes and spheroids is occurring in concert through mergers, thus setting the linear relationship. A similar linear relation would hold for the final black-hole masses provided that it has not been changed by the subsequent growth experienced by black holes via accretion. If the accretion is proportional to the mass of the seed, as would be the case for accretion at the Eddington rate, then we expect the slope of the relation to persist. Of course, the effect of accretion depends on what fraction of the black hole mass was accreted. If the increase in mass is only by a factor of a few, then one could assume that the role of mergers in setting the observed relationship is important. On the other hand, if the growth by accretion is by more than an order of magnitude, then the accretion process would have the dominant role in determining the slope of the relation. According to our model, the normalization of the observed relationship is determined additively by two free parameters: the viscous timescale and the growth via accretion. When adopting a physically motivated value for the viscous timescale, we find that growth via accretion is limited to be by an order of magnitude or less, thus suggesting that mergers do play an important role in setting the relationship. We note that in models where the seeds are of smaller masses,  $\sim 100 M_{\odot}$  (e.g., Volonteri, Haardt & Madau 2003), the growth by mergers is negligible and the accretion process has to be tuned with a specific feedback scenario in order to obtain the correct relation between black holes and spheroids.

Although we focused here on black hole and spheroid growth, we do not expect all the seed black holes accreted by a dark matter halo to be incorporated in the spheroid. A number of black holes could be orbiting in haloes of big galaxies. They could have arisen from subhaloes that were disrupted after entering the host halo. Such a scenario has been investigated by Islam et al. (2003a) and the possi-

ble observational consequences are explored in Islam et al. (2003b,c).

## 7 CONCLUSION

We presented a physical model for the production of massive seed black holes at high redshifts, with a characteristic mass  $\sim 10^5 M_\odot$ . We argued that this model provides a useful starting point for explaining the observed relation between the masses of today's black holes and the spheroidal components of galaxies. Massive seeds may also help explain the existence of the supermassive black holes associated with luminous AGN at  $z \gtrsim 6$ .

Our model for seed formation is based on the general idea that the mass in every early-collapsing halo is expected to have a *distribution* of specific angular momentum, with at least some fraction of its gas having a much smaller specific angular momentum than is characterized by the global spin parameter of the halo. After the low-spin gas cools, it can fall into the central region and form a dense disc, where certain viscous processes become effective and may potentially lead to black hole formation.

In our exploration of this idea, we assumed that the specific angular momentum of the gas is similar to that measured for the dark-matter in N-body simulations. In this case, if angular momentum is conserved during the gas infall, the central gas discs become self-gravitating and Toomre unstable in all the haloes above a critical mass. This critical mass has a median value of  $\sim 7 \times 10^7 M_\odot$  at  $z \sim 15$ , and it is expected to be scattered log-normally with a  $\ln$  standard deviation of  $\sim 0.9$ . The sites of seed production are thus much more massive than the typical collapsing mass at that time, and are therefore associated with high-sigma peaks in the fluctuation distribution. Gravitational instabilities in the disc drive an effective viscosity that redistributes angular momentum. As a result, material from the low angular momentum tail of the distribution loses its angular momentum on a viscous timescale and contribute to the formation of a black hole. We associate this viscous timescale with the timescale for disruption and/or heating of the disc due to substantial star formation. We expect this timescale to be on the order of  $1 - 30$  Myr, but its exact value is not well determined.

We found that the typical seed black holes, which form in critical mass haloes, have a characteristic mass of  $\sim 10^5 M_\odot$ , quite insensitive to the epoch of formation. This predicts a lower bound to possible masses of massive black holes, which can be confronted with observations today.

This scenario should operate continuously as additional haloes grow to above the critical mass and create new potential sites for black-hole formation. The process is expected to stop, however, when the Universe becomes sufficiently reionized that  $H_2$  molecules are destroyed and cannot provide efficient cooling. We therefore expect seed black holes to form before  $z_{\text{re}} \sim 13 - 21$ .

We showed that the comoving density of mass in seed black holes grows gradually with time, in association with the birthrate of critical mass haloes. This density becomes comparable to the observed mass density of supermassive black holes by  $z \sim 15$ , near the redshift of reionization. Depending on the adopted viscous timescale, there is room

for an order of magnitude growth in black hole masses via quasar powering accretion. We find that a viscous timescale of  $t \sim 5 - 10$  Myr provides quite reasonable results.

We explored the development of a correlation between black-hole mass and spheroid mass in today's galaxies by tracking our early forming massive seed population through a halo merger tree. Under the assumption that spheroids form via major mergers, we showed that the merger process leads naturally to a linear relation between black-hole mass and spheroid mass. This result is mainly due to the formation of *massive* seeds only in rare, high-peak haloes at high redshifts, and is not too sensitive to the details of our seed formation model. Starting with  $\sim 1 - 100 M_\odot$  seeds would not lead to a linear correlation via mergers alone; additional feedback associated with AGN accretion is needed. The seed black holes in our model have masses that are proportional to the virial masses of their host haloes at formation. We demonstrated that this linear relation is preserved if black holes merge in concert with the hierarchical growth of haloes and spheroids.

One potentially interesting ramification of our scenario is that a population of massive black holes at high redshift might serve to power small quasars, fueled perhaps by low-angular-momentum gas liberated by merger events that occur after the seeds are in place. Madau et al. (2003) discussed how a population of "mini-quasars" like this might be responsible for reionizing the universe at  $z_{\text{re}} \sim 15$ . However, in their model, the mini-quasar power-sources were intermediate-mass  $\sim 100 M_\odot$  black holes. Under similar assumptions, the massive seed black holes of our model would produce even more ionizing photons per site, and perhaps lead more naturally to an early reionization. In our current scenario the reionization epoch was an input parameter detached from the black-hole formation process, but, in principle, the accretion onto the seeds themselves could be responsible for the reionization that eventually inhibits further black-hole formation.

Our quantitative predictions should not be interpreted too literally. For example, our fiducial model assumes that the initial angular-momentum distribution of the gas mirrors that of a typical CDM halo, and that it is preserved during disk formation. There is no evidence in local galaxies for discs with inner densities as high as invoked by our model for proto-galaxies. This might be explained by processes that have altered the gas angular-momentum distribution preferentially at late epochs, such as feedback effects (e.g. Maller & Dekel 2002), but one should clearly assign a substantial degree of uncertainty to our model assumption. In order to address this uncertainty, at least qualitatively, we explored the effect of varying the initial angular momentum distribution. We found that if the low angular momentum tail is as minor as in an exponential disc of a constant-density core ( $\xi = 2$ ), the resulting seed black holes are too small to be of relevance. An intermediate case, with  $\xi = 1.3$ , can produce sensible black-hole seeds, comparable to our fiducial case ( $\xi = 1$ ), provided that the viscosity timescale is slightly longer,  $20 \leq t \leq 30$  Myr. For  $\xi = 1.3$ , the critical halo mass becomes  $\sim 10^8 M_\odot$  at  $z = 15$ , and the inner  $\sim 10\%$  of the disc mass manages to lose its angular momentum by viscosity and produce a black hole of mass  $\sim 10^6 M_\odot$ . This seed mass is larger than in the fiducial case, but the seeds in this case are rarer events (see figure 3.1).

Therefore, in order to recover a similar total mass density in black holes, the viscosity must operate for a longer duration. The actual low angular-momentum tail of the gas distribution remains an unknown, which will hopefully be constrained by future, more realistic hydrodynamical simulations, properly including feedback and other important physical effects.

In conclusion, while the model presented here is clearly idealized, it does provide a useful example for the kind of mechanism needed to connect cosmological structure formation on galactic scales to black-hole formation on much smaller scales. Observations suggest the presence of massive black holes at high redshifts and therefore the need for the formation of massive seed black holes at still earlier times. According to our scenario, the observed correlations of black hole and galaxy properties are directly linked to the hierarchical nature of structure formation itself, and owe their existence to rare systems forming in association with the first light.

## 8 ACKNOWLEDGMENTS

We acknowledge stimulating comments from Martin Haehnelt, Paul Martini, Eve Ostriker, Martin Rees, Brant Robertson, David Weinberg, Terry Walker and Andrew Zentner. We thank the anonymous referee for helpful suggestions that improved the quality of this article. SMK thanks the 2003 Santa Fe cosmology workshop where part of this work was completed. AD thanks the IAP, Paris, for their hospitality. This work has been supported by U.S.DOE Contract No. DE-FG02-91ER40690 (SMK), NASA Hubble Fellowship grant HF-01146.01-A (JSB), and ISF grant 213/02 (AD).

## REFERENCES

- Abel T., Anninos P., Norman M. L., Zhang Y., 1998, *ApJ*, 508, 518
- Adams F. C., Graff D. S., Richstone D. O., 2001, *ApJ*, 551, L31
- Adams F. C., Graff D. S., Mbonye M., Richstone D. O., *astro-ph/0304004*
- Barafee I., Heger A. & Woosley S. E., 2001, *ApJ*, 550, 890
- Barkana R. & Loeb A., 2001, *Phys. Reports*, 349, 125
- Barnes J., Efstathiou G., 1987, *ApJ*, 319, 575
- Barth A. J., Martini P., Nelson C. H., Ho L. C., 2003, *ApJ*, 594, L95
- Binney J., Tremaine S., 1987, *Galactic Dynamics*. Princeton Univ. Press, NJ
- Birnboim Y., Dekel A., 2003, *MNRAS*, 345, 349
- Bond J. R., Cole S., Efstathiou G., Kaiser N., 1991, *ApJ*, 379, 440
- Bromley J. M., Somerville R. S., Fabian A. C., *astro-ph/0311008*
- Bromm V., Loeb A., 2002, *astro-ph/0212400*
- Bryan G. L., Norman M. L., 1998, *ApJ*, 495, 80
- Bullock J. S., Kravtsov A. V., Weinberg D. H., 2000, *ApJ*, 539, 517
- Bullock J. S., Dekel A., Kolatt T. S., Kravtsov A. V., Klypin A. A., Porciani C., Primack J. R., 2001a, *ApJ*, 555, 240 (B01)
- Bullock J. S., Kolatt T. S., Sigad Y., Somerville R. S., Kravtsov A. V., Klypin A. A., Primack J. R., Dekel A., 2001b, *MNRAS*, 321, 559
- Bullock J. S., Kravtsov A. V., Colín P., 2002, *ApJ*, 564, L1
- Chen D. N., Jing Y. P., 2002, *MNRAS*, 335, L89
- Chen D. N., Jing Y. P., Yoshikawa K., 2003, *ApJ*, 597, 35
- Chokshi A., Turner E. L., 1992, *MNRAS*, 259, 421
- Colín P., Avila-Reese V., Velanzuela O., Firmani O., 2002, *ApJ*, 581, 777
- Colpi M., Mayer L & Governato F., 1999, *ApJ*, 525, 720
- Dekel A., Silk J., 1986, *ApJ*, 303, 39
- Dekel A., Woo J., 2003, *MNRAS*, 344, 1131
- Dekel A. et al., 2001, in Funes J. G., S. J., Corsini E. M., eds, *Galaxy discs and disc galaxies*
- Ebisuzaki T., Makino J., Tsuru T., Funato Y., Portegies Z. S., Hut P., McMillan S., Matsushita S., Matsumoto H., Kawabe R., 2001, *ApJ*, 552, L19
- Eisenstein D. J., Loeb A., 1995a, *ApJ*, 443, 11
- Eisenstein D. J., Loeb A., 1995b, *ApJ*, 439, 520
- Fabian A. C., Iwasawa K., 1999, *MNRAS*, 303, L34
- Fan X., Strauss M. A., Schneider D. P., Gunn J. E., Lupton R. H., Becker R. H., Davis M., Newman, J. A., Richards G. T., White R. L., Anderson J. E. Jr., Annis, J., Bahcall N. A., Brunner R. J., Csabai I., Hennessy G. S., Hindsley R. B., Fukugita M., Kunszt P. Z., Ivezić Z., Knapp G. R., McKay T. A., Munn J. A., Pier J. R., Szalay A. S., York D. G., 2001, *AJ*, 121, 54
- Ferrarese, L. & Merritt, D., 2000, *ApJ*, 539, L9
- Gebhardt K., Lauer T. R., Kormendy J., Pinkney J., Bower G. A., Green R., Gull T., Hutchings J. B., Kaiser M. E., Nelson C. H., Richstone D., Weistrop D., 2001, *AJ*, 122, 2469
- Ghigna S., Moore B., Governato F., Lake G., Quinn T., Stadel J., 1998, *MNRAS*, 300, 146
- Gnedin O. Y., 2001, *Class. & Quant. Grav.*, 18, 3983
- Haehnelt M. G., Rees M. J., 1993, *MNRAS*, 263, 168
- Haehnelt M. G., Natarajan P., Rees M. J., 1998, *MNRAS*, 300, 827
- Haiman Z., Loeb A., 2001, *ApJ*, 552, 459
- Hawking S. W., 1971, *MNRAS*, 152, 75
- Hawking S. W., 1971, *PRL* 26, 1344
- Heger A., Woosley S. E., 2002, *ApJ*, 567, 532
- Hills D., Bender P. L., 1995, *ApJL*, 445, 7
- Hoyle F., 1949, *IAU and International Union of Theoretical and Applied Mechanics Symposium*, p.195
- Islam R. R., Taylor J. E., Silk J., *astro-ph/0307171*
- Islam R. R., Taylor J. E., Silk J., *astro-ph/0309558*
- Islam R. R., Taylor J. E., Silk J., *astro-ph/0309559*
- Kauffmann G., Haehnelt M. G., 2000, *MNRAS*, 311, 576
- Klypin A., Zhao H., Somerville R. S., 2002, *ApJ*, 573, 597
- Kormendy J., Richstone D., 1995, *ARA&A*, 33, 581
- Kormendy J., Gebhardt K., 2001, *astro-ph 0105230*
- Lacey C., Cole S., 1993, *MNRAS*, 262, 627.
- Laughlin G., Rozyczka M., 1996, *ApJ*, 456, 279L
- Lee H. M., 1995, *MNRAS*, 272, 605
- Lin D. N. C., Pringle J. E., 1987, *MNRAS*, 225, 607
- Loeb A., Rasio F. A., 1994, *ApJ*, 432, 52
- Madau P. & Rees M. J., 2001, *ApJ*, 551, L27
- Madau P., Rees M. J., Volonteri, M., Haardt, F., Oh, S. P., 2003, *astro-ph/0310223*



- Magorrian J., et al., 1998, *AJ*, 115, 2285
- Maller, A., Dekel, A., 2002, *MNRAS* 335, 487
- Maller, A., Dekel, A., Somerville R., 2002, *MNRAS* 329 423
- Martini P., Weinberg D. H., 2001, *ApJ*, 547, 12
- Martini P., 2003, *astro-ph/0304009*
- Menou, K, Haiman, Z, Vijay, K. N., 2001, *ApJ* 558, 535
- Merritt D., Ferrarese L., 2001, *MNRAS*, 30, 320L
- Mineshige S., Umemura M., 1997, *ApJ*, 480, 167
- Peebles P. J. E., 1969, *ApJ*, 155, 393
- Porciani C., Dekel A., Hoffman Y., 2002a, *MNRAS*, 332, 325
- Porciani C., Dekel A., Hoffman Y., 2002b, *MNRAS*, 332, 339
- Press W. H., Schechter P., 1974, *ApJ*, 187, 425
- Quinlan G. D., Shapiro S. L., 1990, *ApJ*, 356, 483
- Salucci P., Szuszkiewicz E., Monaco P., Danese L., 1999, *MNRAS*, 307, 637
- Shaerer D., 2002, *A&A*, 382, 28
- Shakura N. I., Sunyaev R. A., 1973, *A&A*, 24, 337
- Shapiro S. L., Teukolsky S. A., 1983, *Black holes, white dwarfs and neutron stars*, Wiley, NY
- Shapiro S. L., Shibata M., 2002, *ApJ*, 577, 904
- Sharma P., Steinmetz P., *astro-ph/0406533*
- Shaviv, N. & Dekel, A., 2004, *astro-ph/0305527*
- Soltan A., 1982, *MNRAS*, 200, 115
- Somerville R. S. & Kolatt T., 1999, *MNRAS*, 305, 1
- Spergel D. N., Verde L., Peiris H. V., Komatsu E., Nolte M. R., Bennett C. L., Halpern M., Hinshaw G., Jarosik N., Kohut A., Limon M., Meyer S. S., Page L., Tucker G. S., Weiland J. L., Wollack E., Wright E. L., 2003, *ApJS*, 148, 175
- Steed A., Weinberg D. H., 2003, in preparation
- Taylor J. E., Babul A., 2001, *ApJ*, 559, 716
- Taylor J. E., Babul A., *astro-ph/0301612*
- Tegmark M., Silk J., Rees M. J., Blanchard A., Abel T., Palla F., 1997, *ApJ*, 474, 1
- Toomre A., 1964, *ApJ*, 139, 1217
- Tormen G., 1997, *MNRAS*, 290, 411
- Tremaine S., Gebhardt K., Bender R., Bower G., Dressler A., Faber S. M., Filippenko A., Green R., Grillmair C., Ho L. C., Kormendy J., Lauer T. R., Magorrian J., Pinkney J., Richstone D., 2002, *ApJ*, 574, 740
- van der Marel R. P., 1991, *MNRAS*, 253, 710
- van den Bosch F. C., Lewis G. F., Lake G., Stadel J., 1999, *ApJ*, 515, 50
- van den Bosch F. C., Burkert A., Swaters R. A., 2001, *MNRAS*, 326, 1250
- van den Bosch F. C., Abel T., Croft R. A. C., Hernquist L., White S. D. M., 2002, *ApJ*, 576, 21
- Volonteri M., Haardt F. & Madau P., 2003, *ApJ*, 582, 559
- Yu Q., Tremaine, 2002, *MNRAS*, 335, 965
- Zentner A. R., Bullock J. S., 2003, *ApJ*, 598, 49